buildings

MDPI

Article

An Evaluation of Mechanical Properties of Nano GGBFS in Concrete with Statistical Validation

Johnpaul Vincent [1,*], Balasundaram Natarajan [1], Daniel Das Amaladas [2] and Daniel Cruze [3,*]

[1] Department of Civil Engineering, Karpagam Academy of Higher Education, Coimbatore 641021, Tamil Nadu, India; balasundaram.n@kahedu.edu.in
[2] Department of Mechanical Engineering, Karpagam Academy of Higher Education, Coimbatore 641021, Tamil Nadu, India; danielamaladas@gmail.com
[3] Department of Civil Engineering, Hindustan Institute of Technology and Science, Chennai 603103, Tamil Nadu, India
* Correspondence: johnpaulv2490@gmail.com (J.V.); danielckarunya@gmail.com (D.C.); Tel.: +91-9952506549 (J.V.)

Abstract: Concrete, the most extensively utilized construction material, maintains its high demand owing to the swift urbanization and population expansion worldwide. However, cement manufacturing consumes considerable energy and emits substantial CO_2 into the atmosphere. To ensure the construction industry's sustainability, it is imperative to use eco-friendly and cost-effective products. As an additional cementitious ingredient in concrete, nano-based GGBFS (NGGBFS) is therefore employed to provide sustainable environmental impacts. The main purpose of this study is to assess the compressive strength, tensile strength, and Young's modulus of NGGBFS, considering various replacement percentages (2%, 4%, 6%, 8%, 10%, and 12%) compared to conventional cement. The maximum compressive strength (72.68 MPa) and tensile strength (6.12 MPa) were obtained at 365 days for GB4 concrete. The Taguchi optimisation technique was employed to determine the interaction between mineral admixture and curing days on the mechanical properties of concrete; it reveals that GB4 mineral admixture and 365 days of curing days have good interaction between the factors taken for the study. The ANOVA quadratic regression model provided the optimisation process response. According to principal component analysis, the compression strength and Young's modulus significantly influence the components because their loadings are so close (0.722 and 0.68). As a result, optimal combinations with equivalent strengths can be successfully created by substituting 8% nano-based GGBFS (GB4) in cement, offering an alternative path toward sustainable development.

Keywords: ANOVA; compressive strength; optimisation; split tensile strength; Taguchi; Young's modulus

check for updates

Citation: Vincent, J.; Natarajan, B.; Amaladas, D.D.; Cruze, D. An Evaluation of Mechanical Properties of Nano GGBFS in Concrete with Statistical Validation. *Buildings* **2023**, *13*, 3060. https://doi.org/10.3390/buildings13123060

Academic Editor: Giuseppe Santarsiero

Received: 13 October 2023
Revised: 25 November 2023
Accepted: 3 December 2023
Published: 8 December 2023

Copyright: © 2023 by the authors. Licensee MDPI, Basel, Switzerland. This article is an open access article distributed under the terms and conditions of the Creative Commons Attribution (CC BY) license (https://creativecommons.org/licenses/by/4.0/).

1. Introduction

Concrete is an indispensable construction material that has shaped the modern world. The world's annual concrete supply is estimated at around one cubic meter per person on Earth. Each year, the worldwide demand for concrete reaches approximately 11 billion tonnes, making it the primary material used in construction [1]. Concrete is typically composed of a mixture of Portland cement, sand, crushed rock, and water. The consumption of Portland cement in the United States alone has risen significantly, reaching 500 million tonnes, which is five times greater than the amount of steel consumed. Steel–concrete ratios are close to 10^{-1} in most nations. Apart from water, there is no other substance consumed in such vast quantities as concrete. Concrete usage exhibits regional disparities influenced by economic development, population growth, and construction activities [2]. Concrete production has environmental implications, primarily due to the energy-intensive process of cement manufacturing. Simultaneously, CO_2 emissions from Ordinary Portland

cement production continue to climb yearly due to fossil fuel combustion [3]. Geological polymer cement emits only 0.180 kg of CO_2 per kilogram during its manufacturing process, which is less than one-fifth of the emissions generated by traditional silicate cement [4]. This highlights the importance of using sustainable construction materials to mitigate environmental damage. Geopolymers and alkali-activated binders are considered environmentally friendly alternatives to conventional binding materials, as they have minimal ecological impact.

All cement alternatives can substitute energy-intensive Portland cement while repurposing material that would otherwise be disposed of in landfills. The production of Portland cement is responsible for approximately 7% of global carbon emissions, significantly contributing to global warming. To promote sustainable development in the construction industry, it is crucial to explore alternative solutions with favourable characteristics. Ground Granulated Blast Furnace Slag (GGBFS) is a by-product of the iron and steel industry, obtained by rapidly cooling molten iron slag from a blast furnace with water or steam [5]. GGBFS is commonly used as a supplementary cementitious material (SCM) in concrete mixtures, alongside Portland cement. The compressive strength of concrete is affected by four major factors: specimen size, shape, pores, and friction between the specimen surfaces. Concrete pores can be categorized into three main types: gel, capillary, and air voids [6]. In order to enhance the microstructure of the hydrated cement paste and reduce the presence of pores, a strategy involving the partial replacement of cement weight needs to be employed in the concrete matrix. Nano-based ground granulated blast furnace slag along with mineral admixtures can be utilized to improve the overall quality and characteristics of the cement paste surrounding the particle by using the materials [6–8].

Nanomaterials, ultrafine particles, are being employed to modify concrete, significantly enhancing its mechanical and deformation properties. Incorporating nanoparticles into the concrete matrix serves multiple roles, such as improving the microstructure as fillers, promoting pozzolanic reactions as activators, acting as nucleation sites for CSH seeds, and expediting the formation of C3S and CH crystals. The inclusion of nano considerably boosted early strength at 7 days. Ref. [9] worked with a different percentage of nano blast furnace slag in concrete as a substitute for cement. Mechanical durability provides ASTM (American Society for Testing and Materials) standards that have been tested for hardened concrete specimens. In a study conducted [10] the effects of incorporating micro-silica and nano-silica in concrete were investigated. The researchers examined different percentages of micro-silica and nano-silica, ranging from 0% to 15%. They found that 5% nano-silica was the optimal percentage for achieving desirable outcomes. Additionally, they conducted fly ash replacements at various levels, and it was observed that a 30% replacement was satisfactory for achieving enhanced strength with the addition of the optimal dose of nano-silica. Ref. [11] concentrated mainly on testing the hardened material's strength when the wearing stage is converted into the grosser cemented matrix, the monomer molecules' reaction rate forms the C-S-H gel's silicate chain [12]. Nano-clay SCC (self-consolidating concrete) specimens from the mineral additives successfully meet the demands of hardness and durability parameters. The new mixing status is also workable in compliance with EFNARC (European Federation for Specialist Construction Chemicals and Concrete Systems) requirements.

Typically, challenges involving numerous variables have been tackled using the "one variable at a time" (OVAT) technique, which is accomplished through the design of experiments (DoE). Applications of DoE in concrete studies include creating concrete mix designs to predict concrete strength. Since the strength of concrete cannot be inferred from the results of non-destructive testing, the assessment of concrete strength through these tests sometimes necessitates a mathematical calculation [13]. The long-term effects of multiwall carbon nanotube content on cement-based composites' compressive and flexural strengths with Weibull distribution functions, the results display distinct trends before and after 28 days. Additionally, the study contrasts European design codes with flexural and compressive strengths [14]. The Taguchi technique and Response Surface approach

are preferred to streamline the experimental procedure in studies with extensive tests and datasets. Artificial neural networks are a different approach that may be used for sophisticated analysis, especially by researchers familiar with computing concepts [15]. The correlations between the various performance traits of materials vary in strength, and their weights alter depending on the circumstances. To address these shortcomings, principal component analysis (PCA) converts potentially associated responses into Unassociated main components. Principal Component Analysis (PCA) is a powerful technique used to identify correlated patterns in data and uncover similarities and differences within the dataset [16]. The fundamental concept behind PCA is to identify the primary components of the original data and subsequently reduce its dimensionality. By doing so, PCA enables the compression of the data into a smaller set of principal components.

The objective of the present research was to investigate the effects of incorporating nano GGBFS as a partial replacement for cement in concrete. The study focused on evaluating the impact of NGGBFS replacement on various mechanical properties, including workability, compressive strength, tensile strength, and Young's modulus through experimental analysis. Additionally, the study aimed to determine the optimal levels of two key factors, namely curing days and mineral admixture, utilizing Taguchi's method. For each parameter, like curing and different mineral admixtures, four levels (curing days: 7, 14, 28 and 365 days; mineral admixture: 0, 2, 8 and 12%) were selected by employing an L16 orthogonal array. Experiments were conducted to investigate the optimum levels of each factor parameter for the responses: compressive, tensile strength and Young's modulus. Using Taguchi's approach, significant factors and their rankings were also determined. The findings of Taguchi's technique and ANOVA were compared to determine the factor parameter with the most minor and most significant effect on the responses and the optimal values of each factor. To predict the ideal setting, this study also combines PCA with Taguchi. This method's projected outcome was confirmed using a confirmatory test, demonstrating the process's effectiveness.

2. Materials and Methods

This study used experimental testing to investigate the mechanical characteristics of concrete. The binder used in this study was Ordinary Portland cement, specifically grade 53, with a specific gravity of 3.15. For the fine aggregate, manufacturing sand was employed, which has a specific gravity of 2.6 and a fineness modulus of 2.7. Samples collected from the study exhibited initial and final setting durations of 120 and 220 min, respectively. GGBFS was sourced from the iron and steel industry and ground to nanoscale using a top-to-bottom technique. It was found to have a chemical composition equivalent to cement, as shown in Table 1, with a specific gravity of 2.98.

Table 1. Chemical properties of GGBFS.

Constituent	GGBFS
CaO (Lime)	47.91
SiO_2 (Silica)	31.35
MgO (Magnesia)	2.59
Al_2O_3 (Alumina)	12.61
Fe_2O_3 (Iron oxide)	1.5
SO_3 (Sulphur trioxide)	0.81
Na_2O (Sodium oxide)	0.95
K_2O (Potassium oxide)	1.30
Loss of ignition	0.98

The GGBFS collected are of different sizes and shapes; since the porosity of concrete can differ due to its physical appearance, it must be rendered into particular dimensions to attain greater strength and durability. So, for size reduction of GGBFS, a Fritsch, GmbH, Germany Pulversitte5 classical line ball mill was used. was used as a water-reducing agent

with a specific gravity of 1.18 @ 25 °C. It was brown, with zero chloride content and less than 2% additional air entrained at standard dosages.

2.1. Workability

The flow of cement mortar was significantly reduced during both replacement stages of GGBFS mortar. The finer the substance, the larger the surface area and, as a result, the more water is required to wet the surface. The mineral admixtures must be added to the mortar appropriately to ensure a satisfactory and viscous fluid structure. The minerals boosted mortar strength, which increased flow and lessened surface tension, resulting in a rise in cement mortar viscosity. The M30 Mix Designs, as characterized by IS10262-2009 [17], are shown in Table 2 with chemical admixture 1.9/m^3.

Table 2. Mix Ratio.

Specification	Cement	Fine Aggregate	Coarse Aggregate	Water Cement Ratio	Reference
Mass in kg/m^3	380	712	1286	160:380	[17]
Ratio	1	1.87	3.38	0.42	

M30 grade concrete with a water–cement ratio of 0.42. Materials were weighed, batched, blended in a revolving drum mixer, cast, and compacted using a vibrating table. The specimens' compressive strength was determined using the BS1139 standards [18]. Seven mixed proportions (CM, GB1, GB2, GB3, GB4, GB5, GB6) were prepared for each test and labelled by the parameters and numbers such that the ingredients were identifiable from their identity document. For instance, the CM was a control mix with a water–cement ratio of 0.42, with no nano mineral admixture.

2.2. Compressive Strength, Split Tensile Strength and Young's Modulus

The compression strength, split tensile strength, and Young's modulus were measured using a compressive measuring system with an ability of 2000 kN for each trial mix mixture. The loading rate of 140 kg/cm^2/min was applied after the specimen had been centred in the measuring machine. The cube specimens of size 150 mm× 150 mm× 150 mm and cylinders of size 150 mm × 300 mm were made to analyse the compressive strength, split tensile strength, and Young's modulus, respectively. The specimens were cast for 7 days, 14 days, 28 days, and 365 days; samples were kept at room temperature for 24 h before being withdrawn from the moulds and cured in normal water.

Because of the dependence of nano mineral admixture concrete on different parameters, the GGBFS curing days and various mineral admixtures were considered two main factors. For each parameter, like curing and different mineral admixtures, in this study, four levels (curing days: 7, 14, 28 and 365 days; mineral admixture: 0, 2, 8 and 12%) were selected.

2.3. Design of Experiments

The components of mixed designs have often been optimised using the Taguchi approach. It is a systematic strategy that reduces testing time and experimental costs. The surroundings and the components used to produce a product, in accordance with Taguchi, determine that product's performance. Maximizing the strength parameters is the key goal. Four variables with four levels are relevant in the current investigation, resulting in 16 possibilities for each blend. This study uses L16 orthogonal arrays (OA) for each mix. The compressive strength, split tensile strength, and Young's GGBFS mix modulus were considered variables for Taguchi analysis using Minitab 16. With the use of PCA, the challenges of combining the various measurement units, discovering the connections between variables, and assuming the weights may be overcome. By employing the Taguchi-based PCA method, the study successfully attained an optimal combination of

mix design factors. To assess the statistical influence of different percentages of NGGBFS on the compressive strength, split tensile strength, and Young's modulus of the concrete samples, an analysis of variance (ANOVA) test was conducted. The significance threshold for the hypothesis test was determined by the probability, or *p*-value, which was set at 0.05. This analysis allowed for a comprehensive evaluation of the effects of NGGBFS on these key mechanical properties. Hence, the experimental data were subjected to a statistical analysis using the Taguchi-based PCA experimental design and multi-regression analysis.

3. Results

The workability was improved by introducing a suitable amount of chemical admixture. The workability properties of concrete are in Table 3.

Table 3. Fresh properties of concrete.

Mix	Slump (mm)	Compaction Factor
CM	100	0.933
GB1	100	0.925
GB2	97	0.921
GB3	97	0.915
GB4	95	0.911
GB5	93	0.903
GB6	90	0.900

The compaction factor test consists of applying a standard amount of work to the expected quality of concrete, and the resulting compaction was measured. The self-compacting concrete is indicated if the compaction factor value is more significant than one. However, our concrete is not self-compacting. The inclusion of nanoparticles in concrete reduced the workability of the material. The shift in a slump might be due to nano admixture having a large surface area, which needs much water to maintain uniformity [19].

3.1. Cube Compressive Strength

It outlines the effects of the compressive evaluation of cubes. Figure 1 depicts the variance of compressive intensity with the different blends considered.

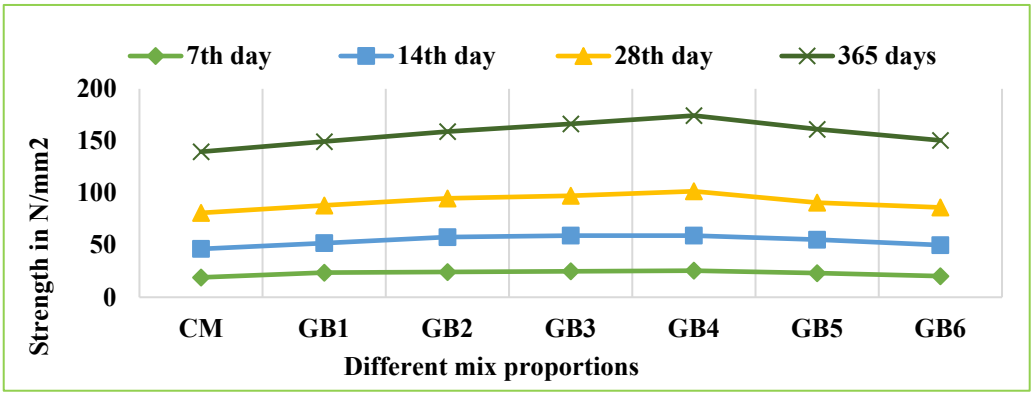


Figure 1. Comparison of cube compressive strength.

The results of the study revealed a significant increase (18.65%) in compressive strength for the GB4 concrete mix compared to the control mix after 28 days of curing. The findings also demonstrated that the GB4 concrete exhibited a maximum compressive strength of 72.68 MPa after 365 days of curing. In a related case study conducted by [20] on self-compacting geopolymer concrete, it was observed that increasing the concentration of GGBFS along with nano-silica in each concrete mix resulted in improved compressive strength. This indicates the positive impact of incorporating GGBFS and nano-silica on

enhancing the compressive strength of the concrete. Another study by [21] on recycled aggregate concrete using nano-silica discovered nanoparticles might increase the micro-hardness of the concrete's interfacial transition zone by enhancing its mechanical qualities like compressive strength and durability properties and favouring corrosion resistance.

3.2. Cylinder Compressive Strength

Figure 2 presents the tabulated results of the compressive strength tests conducted on cylinders, showcasing the variation in compressive strength across different concrete mixes. The analysis revealed a substantial 40.76% increase in compressive strength for the GB4 concrete mix after 28 days of curing, in comparison to the control mix. Additionally, the highest compressive strength of 51.60 MPa was achieved after 365 days of curing for the GB4 concrete mix, surpassing the compressive strength obtained for the control mix. These findings highlight the superior performance of the GB4 mix in terms of compressive strength compared to the control mix. Because of the specific surface area and fineness caused by the incorporated nanoparticles, the increase in compressive strength can be validated by seeding and filler effects [22]. The compressive strength of GB5 and GB6 (35.58 and 36.18 MPa) gradually decreased but did not fall below the compressive strength of the control mix (CM).

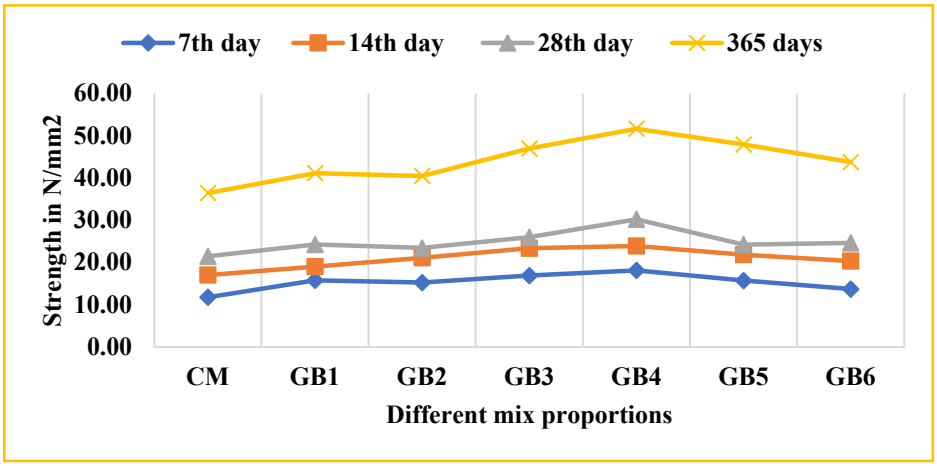


Figure 2. Compressive strength.

According to BS 1881, concrete specimens in the shape of cylinders increase their compressive strength by an amount that is 0.8 times more than that of concrete specimens in the shape of cubes. In this regard, the experiment was carried out to determine if the compressive strength of nano-based concrete exceeded the limit when tested on cylinder and cube specimens. Cube specimens are commonly expected to yield 20–25% greater concrete compressive strength than conventional concrete, with a decreasing variation with more significant or increased compressive strength [23]. Figures 1 and 2 illustrate that, up to a certain point, the addition of nanoparticles boosts compressive strength and achieves its maximum (GB4). Still, after that point, strength begins to decline (GB5 and GB6).

This could be due to CSH gel formation being prevented by the disappearance of $Ca(OH)_2$. After the ideal dose of nanoparticles, it no longer effectively increases the compressive strength of the concrete and merely acts as a pore-refining agent. Moreover, too much silica in concrete causes CSH to change into tobermorite (poor compressive strength substance), which reduces the strength parameter [24].

3.3. Split Tensile Strength

After curing, regular cylinder specimens of scale 150 × 300 mm were cast and checked. The split tensile test findings are tabulated in Figure 3, depicting the split tensile intensity for the different mixes.

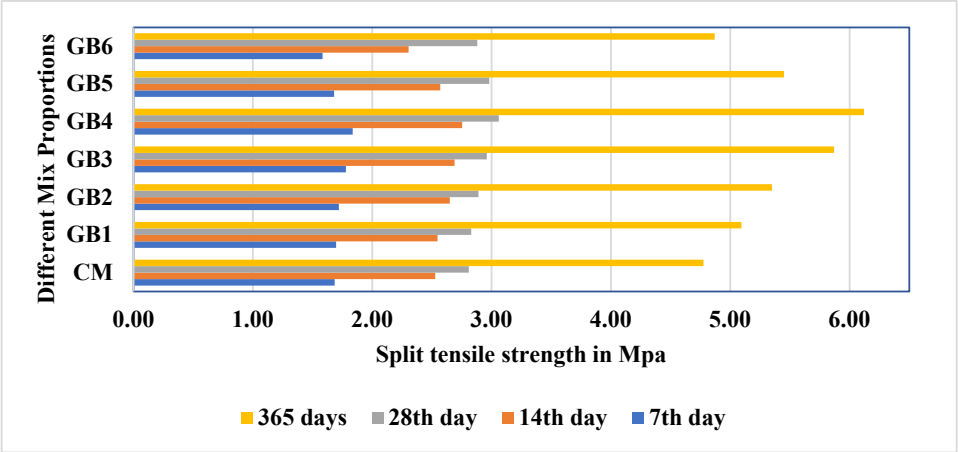


Figure 3. Split tensile strength of concrete.

The study's findings indicate that the GB4 mix exhibited higher split tensile strength compared to the control mix at both 28 and 365 days. Specifically, at 365 days, the GB4 mix demonstrated a maximum split tensile strength of 6.12 MPa. The results are consistent with a study conducted by Oyebisi et al. in 2020, which also observed an increase in splitting tensile strength with longer curing periods. Furthermore, the tensile splitting strengths were enhanced as the concentration of GGBFS and nano in the mix increased [25]. Splitting tensile strength for nano-based concrete was examined by [26], who stated that the tensile strength of nano-modified concrete was increased by 16.10% above that of regular concrete when 3% nanoparticle was used in place of cement. In a study conducted by [27], indirect tensile strength measurements were employed to assess the effect of nano silicate replacement on blended white cement pastes in comparison to the control paste. It was found to be enhanced by roughly 40% when the replacement content of nano silicate was increased to 2%. Also, blended white cement pastes have greater porosity and water absorption rate when replacement content rises.

3.4. Stress–Strain Behaviour of Concrete

The modulus of elasticity test findings is summarised in Table 4. For standard-strength concrete, the strain-to-ultimate stress ratio is usually around 0.003.

Table 4. Modulus of elasticity of concrete.

Replacement of Cement with Nano GGBFS	Modulus of Elasticity Ec (Mpa)	
	Experimental Value in N/mm^2 at 28 Days of Curing	Theoretical $5000\sqrt{fck}$ N/mm^2
CM	24.24	29.40
GB1	26.406	30.07
GB2	27.141	30.48
GB3	28.026	30.90
GB4	29.814	32.60
GB5	27.065	29.82
GB6	27.18	28.80

Post-peak ends in catastrophic loss, with a load of approximately 0.005. As concrete's strength increases, its brittleness decreases, resulting in a reduction in strain failure; the stress–strain graphs are shown in Figure 4.

The study by [12] depicted that the modulus of elasticity decreases for 2% and 3% nano-incorporated specimens by about 25.3% and 15.1%, respectively. However, in this study, the 8% nano admixture showed more of an increased modulus of elasticity (8.5%) than other nano admixtures [12]. In another study by [28] the permeability of plastic

concrete reduces as specimen ageing rises while compressive strength and elastic modulus increase. Moreover, adding nano-silica improves the concrete's compressive strength and dramatically reduces its permeability while maintaining a constant elastic modulus. Young's modulus enhancement is caused by two factors: the intrinsic surface stress and the average lattice compression of nanocrystals. The shift in elastic and vibration behaviour is also influenced by the average atomic binding depth, brought on by the high surface ratio and inherent small size effect [29].

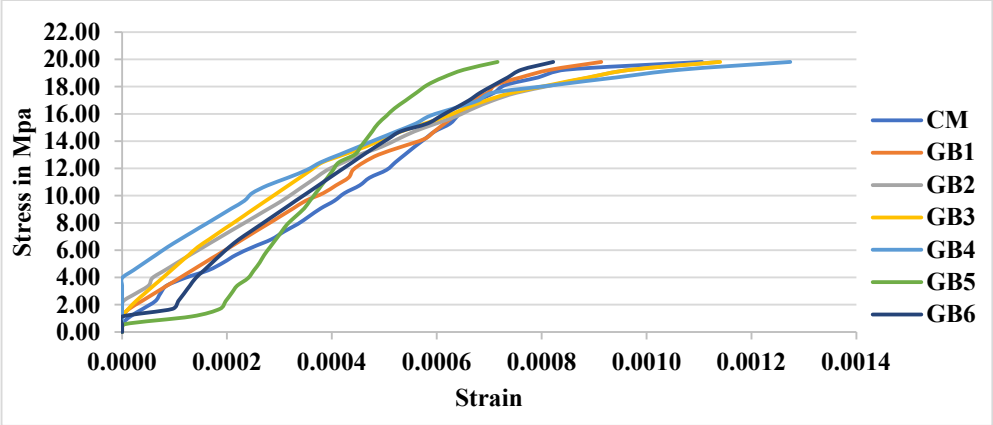


Figure 4. Compressive stress–strain behaviour.

3.5. Design of Experiments

The experimental programme involves:

- Selecting parameters and their levels;
- Choosing an appropriate orthogonal array;
- Conducting experiments;
- Calculating the signal-to-noise ratio (S/N);
- Adopting the Taguchi method to optimise the multiple properties simultaneously.

By employing the Taguchi experimental method, the most significant feasible values of mix proportions were investigated to achieve the highest compressive, splitting tensile, and young modulus for nano GGBFS. To maximize the mechanical qualities of NGGBFS, the "larger-the-better" condition was adopted. Table 5 shows the selected features and their associated levels, empirical series for the L16 orthogonal array using the Taguchi experimental design technique for compressive strength parameters.

Table 5. Taguchi design data.

Different Mineral Admixture Percentage	No. of Days Curing
0	7
0	14
0	28
0	365
2	7
2	14
2	28
2	365
8	7
8	14
8	28
8	365
12	7
12	14
12	28
12	365

3.6. Compressive Strength

The impact of each component on compressive strength improvement was depicted in Figure 5, developed by examining the data in Table 6 and making conclusions from it.

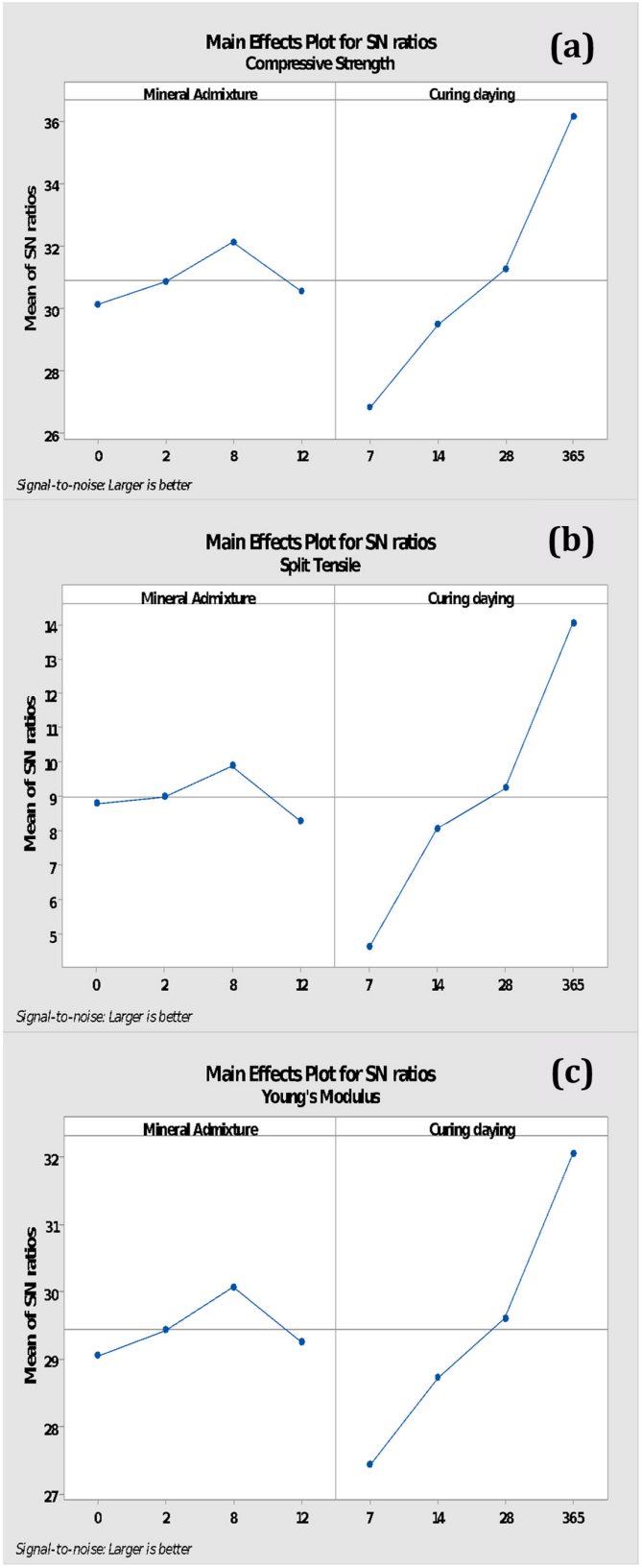


Figure 5. SNR curves on the response: (**a**) compressive Strength; (**b**) spilt tensile; (**c**) Young's modulus.

Table 6. Analysis of variance.

	Source	DF	Adj SS	Adj MS	F-Value	*p*-Value
Compressive strength	Mineral Admixture	3	169.11	56.37		0.002
	Curing Days	3	4054.35	1351.45	290.29	0.000
	Error	9	41.90	4.66		-
	Total	15	4265.36	-		-
Young's modulus	Mineral Admixture	3	27.690	9.230	17.49	0.000
	Curing Days	3	600.075	200.025	378.95	0.000
	Error	9	4.751	0.528	-	-
	Total	15	632.516	-	-	-
Split Tensile	Mineral Admixture	3	0.9660	0.3220	3.02	0.086
	Curing Days	3	24.8854	8.2951	77.85	0.000
	Error	9	0.9589	0.1065	-	-
	Total	15	26.8103	-	-	-

The S/N ratio (SNR) response was determined through an analysis of compressive strength values, as presented in Table 6. The highest rank is denoted by the value 1. According to Table 6, the delta value for the mineral admixture was 1.02, while the delta value for the curing days was 4.63. Figure 6 illustrates the main effect plot for compressive strength. The results indicate that, in comparison to the mineral admixture, the curing days of concrete appeared to significantly influence the progression of compressive strength. According to the Taguchi method, the compressive strength results of NGGBFS mixes (GB2, GB4, and GB8) revealed that GB4 (8% replacement) exhibited the highest compressive strength of 72.68 N/mm^2 after 365 curing days. In contrast, the CM showed the lowest compressive strength after 365 days, approximately 58.71 N/mm^2. The compressive strength S/N ratio for the NGGBFS mix increased significantly with increasing curing days until 8% nano admixture; after this point, it started to decline. This decline may be attributed to the calcium component of GGFBS accelerating polymerization due to the generated heat, thereby facilitating a better polymerization reaction and the gradual formation of CSH structures. These factors contributed to the growth of compressive strength [4].

3.7. Tensile Strength

As indicated in Table 7, the split tensile strength value was also used to compute the S/N ratios response for NGGBFS.

Table 7. Regression response result.

Source	S	R-sq	R-sq (adj)	Equation
Compressive strength	2.15	99.02%	98.36%	26.15 + 0.284 MA+ 0.1012 CD
Spilt tensile	0.33	96.42%	94.04%	2.253 − 0.0027 MA+ 0.007859 CD
Young's modulus	0.73	99.25%	98.75%	25.75 + 0.106 MA + 0.03807 CD
Compressive strength	2.15	99.02%	98.36%	26.15 + 0.284 MA+ 0.1012 CD
Spilt Tensile	0.33	96.42%	94.04%	2.253 − 0.0027 MA+ 0.007859 CD
Young's modulus	0.73	99.25%	98.75%	25.75 + 0.106 MA + 0.03807 CD
Compressive strength	2.15	99.02%	98.36%	26.15 + 0.284 MA+ 0.1012 CD

With a delta value of 9.44, the curing days have the highest position per Table 8, surpassing mineral admixture (delta = 1.596). The tensile strength was significantly influenced by variations in the curing days and mineral admixture, as seen by the plot shapes (Figure 6) for these variables.

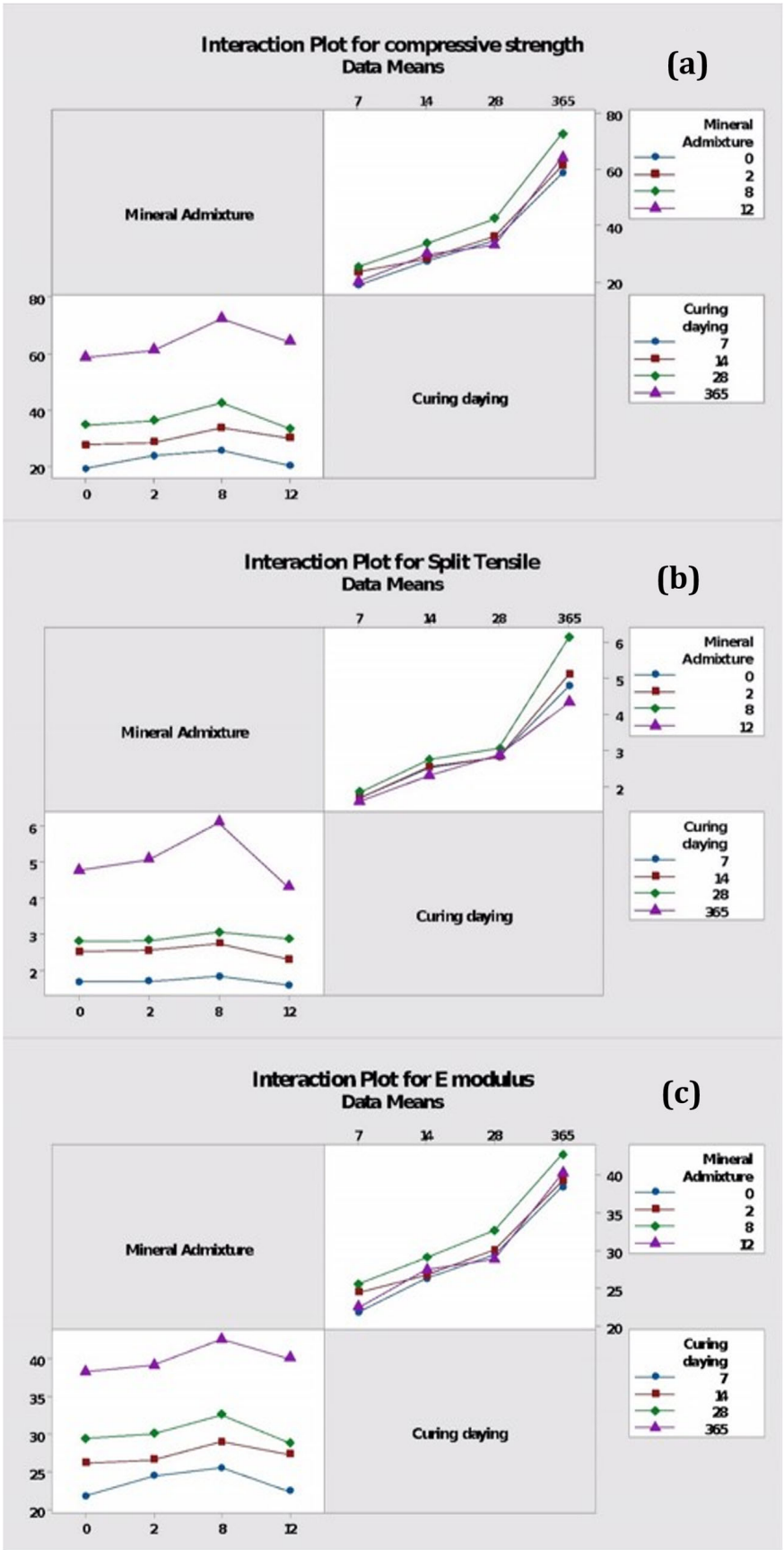


Figure 6. Interaction plot of (**a**) compressive strength; (**b**) split tensile; and (**c**) Young's modulus with two different factors.

Table 8. Percentage contribution of two factors in concrete.

Source	Mineral Admixture	Curing Days	Total	% Contribution—Mineral Admixture	% Contribution—Curing Days
Compressive strength	169.11	4054.35	4265.36	3.96	95.09
Young's modulus	27.690	600.075	632.516	4.38	94.87
Spilt tensile	0.9660	24.8854	26.8103	3.89	92.82

The tensile strength of the concrete samples was observed to improve with an increase in curing days, as indicated by the S/N Ratio analysis. The impact of mineral admixture on split tensile strength decreased when NGGBFS was replaced by 12% (GB8 mix). However, the addition of a nano admixture (GB4 mix) at a specific level resulted in a significant enhancement in splitting tensile strength. This improvement can be attributed to the enhanced interfacial transition zone and the denser, tighter structure of the CSH gels, which contribute to improved splitting tensile strength characteristics [30].

3.8. Young's Modulus

The curing days were a significant factor with a delta value of 4.63 impacting the elastic modulus of concrete, as shown by the mean S/N ratio of the elastic modulus factors and the elastic modulus S/N response diagram of Figure 6. The ratio of the three fundamental components of concrete aggregate, cement paste, and the interface transition zone determines the material's elastic modulus. The key factor contributing to the enhanced elastic modulus of concrete was the inclusion of nanoparticles, which promoted cement hydration. More significant amounts of nanoparticles were more likely to clump together, impeding concrete dispersion. Because of this, the mechanical characteristics of concrete somewhat decreased when nanomaterials were added in quantities higher than recommended [31,32].

The interactive plot for each factor shown in Figure 6 represents that the horizontal lines of mineral admixture 2%, 4%, and 12% were parallel. In contrast, the 8% admixture was not parallel to other factors. The line representing 365 days of curing differed from levels 7, 14, and 28, visualised in the interactive plot for curing days. Hence, it indicates that the GB4 mineral admixture and 365 days of curing days have good interaction between the factors taken for the study.

3.9. ANOVA

MINITAB software 21 was used to analyse the test data using the ANOVA method, with a significance level of 0.05. The statistically significant components were determined via statistical analysis. The degree to which each component contributes to the assessed response indicates its success. It is worth mentioning that the higher a component's contribution percentage, the more probable its variation will produce more changes in that reaction, and it will be regarded as an essential factor. On the other hand, a minor contribution percent indicates that the component has a more negligible effect on the measured response.

An Analysis of Variance (ANOVA) (Table 7) was performed to determine the best percentage of contribution (% of C) or the effect of the individual parameter effect on the compressive strength value. The outcome indicated that the curing days contribute 95.09% to the compressive strength value and are the most powerful influencing factor. Mixture admixture has an insignificant percentage contribution of 3.96%. This model's validity is confirmed by the high R-sq and R-sq adj values, 99.02% and 98.36%, respectively. The percentage contribution of each parameter's influence on split tensile strength and Young's modulus was also determined using an ANOVA (Table 6). The analysis indicates that mineral admixture is an insufficient parameter in both cases, and 365 days of curing was considered the solid influencing factor, accounting for 92.82% and 94.87% of the split tensile strength and Young's modulus, respectively.

3.10. PCA

Using the linear combination of each response parameter, principal components analysis (PCA) was performed to elucidate the nature of variance and covariance. Qj was calculated using main components analysis in this study (PCA). The eigenvalues against the PC count were plotted to obtain the screen plot (Figure 7).

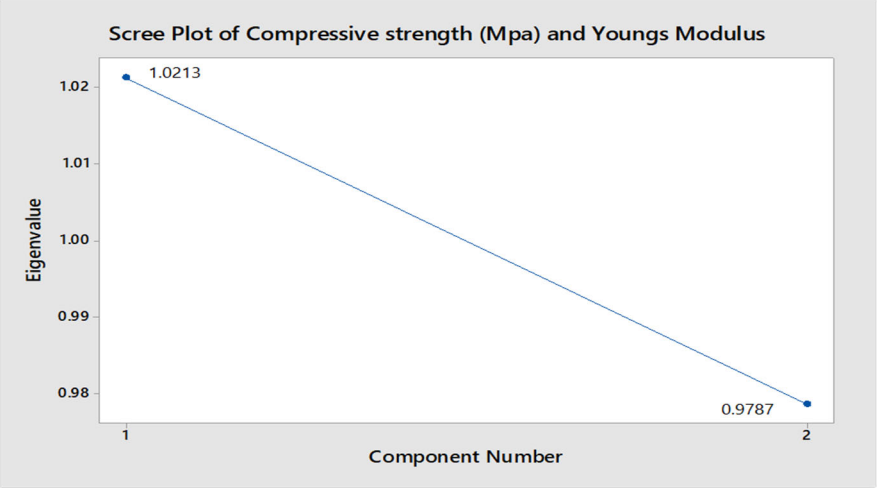


Figure 7. Screen plot of compressive strength and Young's modulus.

The eigenvalues are displayed graphically in decreasing order of magnitude. According to this analysis, the first principal component's eigenvalue was roughly 1.0213, while the second's eigenvalue was approximately 0.9787. Scree Plot indicates that the eigenvalues of the correlation matrix may be equal to the variances of the significant features. The distance between the first and second main components was about 0.511 standard deviations. In contrast, the distance between the second principal components was 0.489 standard deviations. Since PC1 was greater than PC2, its eigenvalue was higher. Thus, the first significant component was used in this investigation. The Mahalanobis distance between each observation and the best-fit line was calculated to identify the outliers (Figure 8).

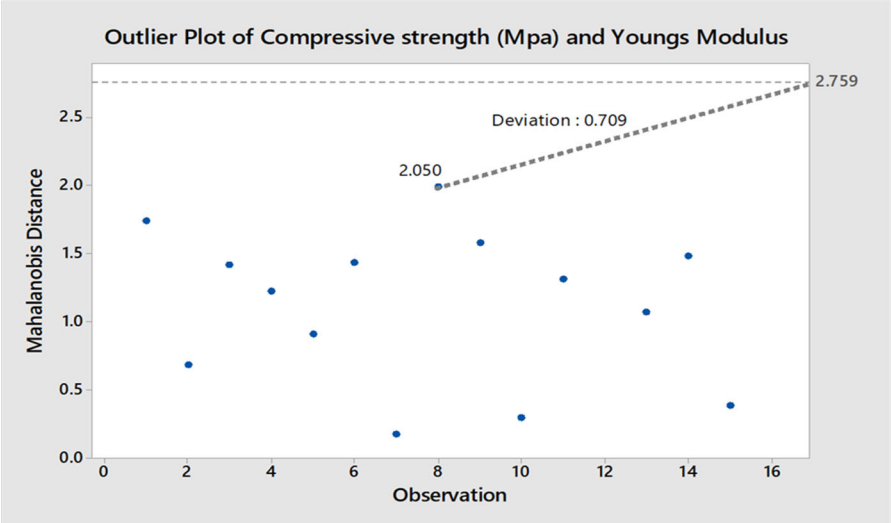


Figure 8. Outlier plot of compressive strength and Young's modulus.

The distance between two points in a multidimensional space was determined. Based on an Outlier Plot analysis, the value of the reference line was identified to be 2.759. The strange point was closer to the reference plot at run number 8. Consequently, everything

was below the zero line. The score plot and the loading plot in a biplot require familiarity with PC data structures and loadings. To see how far off the PCs are from one another, we made a score plot going from the first PC to the second PC using Biplots. A loading plot has been constructed between each variable's coefficient in the first component and the coefficient in the second component. Loadings close to −1 and +1 have an outsized effect on the component. In contrast, loadings close to 0 imply the variable plays a minor role. Biplots, which display the loadings of compression strength and Young's modulus, show that these factors substantially impact the components because their loadings are so near (0.722 and 0.68), respectively (Figure 9).

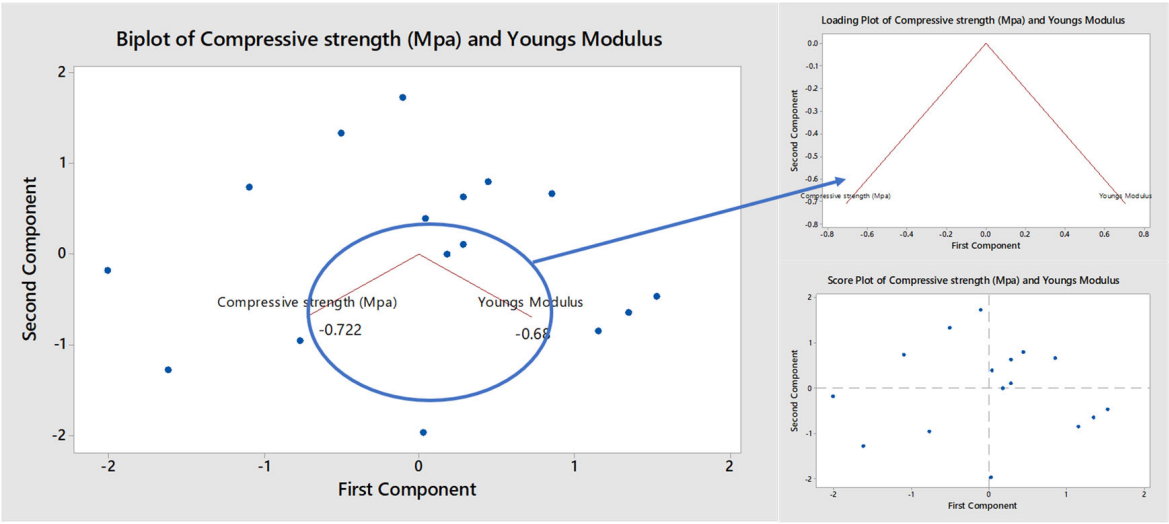


Figure 9. Biplot of compressive strength and Young's modulus.

4. Conclusions

This work investigates the PCA-aided Taguchi optimisation approach to determine the best control parameter settings for the GGBFS with nanoparticle incorporation on the selected responses: compressive, split tensile strength, and Young's modulus. Mineral admixtures and curing days are the chosen regulating factors. Additionally, research was carried out to ascertain Taguchi's factors' percentage contributions and ranking in importance. Through ANOVA, the reliability of the results was examined. The results of the current investigation led to the following conclusions.

- According to the findings, the maximum compressive strength of 72.68 MPa was obtained at 365 days for GB4 mix concrete.
- The average correlation between cube and cylinder compressive strength was found to be 0.709. However, it was observed that beyond the GB4 nano mix, there was a slight decrease in the overall strength of the concrete.
- The GB4 mix exhibited the highest split tensile strength among all the tested mixes, retaining its maximum strength value. The observed percentage increase in split tensile strength for the GB4 mix was 40.76%. Furthermore, the modulus of elasticity at 28 days showed an increase in the GB4 mix compared to the control mix, indicating improved stiffness and rigidity of the concrete.
- By analysing the L16 orthogonal array, the most convincing parameter for seven different admixtures was the 365-day curing period.
- ANOVA results indicate that the curing days, which contribute 95.09% to the compressive strength value, are the most powerful influencing factors. Mixture admixture has an insignificant percentage contribution of 3.96%.
- The significance of mineral admixture as a parameter was found to be relatively limited in comparison. On the other hand, 365 days of curing emerged as the dominant influential factor, accounting for a substantial portion of 92.82% and 94.87% of the split

tensile strength and Young's modulus, respectively. This highlights the significant impact of extended curing duration on enhancing both the split tensile strength and Young's modulus of the concrete.

- Although the percentage contribution varies numerically, the results from Taguchi and ANOVA are consistent with one another and rank the parameters in the same order.
- Compression strength and Young's modulus in PCA show that these factors substantially impact the components because their loadings are so near (0.722 and 0.68, respectively).

The study, therefore, aids in establishing the ideal ratios of the two variables for the three responses. It contributes to better comprehending how the controlling variables impact the compressive, tensile strength, and Young's modulus. Therefore, the outcomes of the statistical analyses conducted for this study can be used as a guide to determine the vital factor and to select the optimal nano-based GGBFS concrete mix.

Author Contributions: Conceptualization, Methodology, Formal Analysis and Investigation, and Writing—Original Draft Preparation: J.V.; Writing—Review and Editing: D.D.A.; Supervision: B.N.; Editing and Supervision: D.C. All authors have read and agreed to the published version of the manuscript.

Funding: This research received no external funding.

Data Availability Statement: Data is unavailable due to privacy or ethical restrictions.

Conflicts of Interest: The authors declare no conflict of interest.

References

1. Vázquez-Calle, K.; Guillén-Mena, V.; Quesada-Molina, F. Analysis of the Embodied Energy and CO_2 Emissions of Ready-Mixed Concrete: A Case Study in Cuenca, Ecuador. *Materials* **2022**, *15*, 4896. [CrossRef] [PubMed]
2. Pheng, L.S.; Hou, L.S. The Economy and the Construction Industry. *Constr. Qual. Econ. A Study Firm Level* **2019**, 21–54. [CrossRef]
3. Nasir, M.; Johari, M.A.M.; Adesina, A.; Maslehuddin, M.; Yusuf, M.O.; Mijarsh, M.J.A.; Ibrahim, M.; Najamuddin, S.K. Evolution of room-cured alkali-activated silicomanganese fume-based green mortar designed using Taguchi method. *Constr. Build. Mater.* **2021**, *307*, 124970. [CrossRef]
4. Karthik, S. A Taguchi Approach for Optimizing Design Mixture of Geopolymer Concrete Incorporating Fly Ash, Ground Granulated Blast Furnace Slag and Silica Fume. *Crystals* **2021**, *11*, 1279. [CrossRef]
5. Esen, Y.; Orhan, E. Investigation of the effect on the physical and mechanical properties of the dosage of additive in self-consolidating concrete. *KSCE J. Civ. Eng.* **2016**, *20*, 2849–2858. [CrossRef]
6. Yang, F.; Yao, Y.; Wei, J.; Wang, X.; Feng, Z. Estimating the Effect of Vibration Mixing Process on Air Pore Size Distributions in Concrete Using Digital Image Analysis. *Buildings* **2022**, *12*, 1142. [CrossRef]
7. Zhang, P.; Gao, Z.; Wang, J.; Guo, J.; Hu, S.; Ling, Y. Properties of fresh and hardened fly ash/slag based geopolymer concrete: A review. *J. Clean. Prod.* **2020**, *270*, 122389. [CrossRef]
8. Rajendran, L.M.; Vincent, J.; Natarajan, B.; Govindan, V. The Effects of Nano-Based Bio-Carbonates in Superhydrophobic Concrete—A Review. *Buildings* **2023**, *13*, 1354. [CrossRef]
9. Sadawy, M.; Nooman, M.T. Influence of nano-blast furnace slag on microstructure, mechanical and corrosion characteristics of concrete. *Mater. Chem. Phys.* **2020**, *251*, 123092. [CrossRef]
10. Hegazy, T.; Mostafa, K.; Esnaashary Esfahani, M. Hands-On Class Exercise for Efficient Planning and Execution of Modular Construction. *J. Civ. Eng. Educ.* **2020**, *146*, 5020002. [CrossRef]
11. He, Z.; Chen, X.; Cai, X. Influence and mechanism of micro/nano-mineral admixtures on the abrasion resistance of concrete. *Constr. Build. Mater.* **2019**, *197*, 91–98. [CrossRef]
12. Mirgozar Langaroudi, M.A.; Mohammadi, Y. Effect of nano-clay on workability, mechanical, and durability properties of self-consolidating concrete containing mineral admixtures. *Constr. Build. Mater.* **2018**, *191*, 619–634. [CrossRef]
13. Chong, B.W.; Othman, R.; Putra Jaya, R.; Mohd Hasan, M.R.; Sandu, A.V.; Nabiałek, M.; Jeż, B.; Pietrusiewicz, P.; Kwiatkowski, D.; Postawa, P.; et al. Design of Experiment on Concrete Mechanical Properties Prediction: A Critical Review. *Materials* **2021**, *14*, 1866. [CrossRef] [PubMed]
14. Huang, J.; Rodrigue, D.; Guo, P. Flexural and compressive strengths of carbon nanotube reinforced cementitious composites as a function of curing time. *Constr. Build. Mater.* **2022**, *318*, 125996. [CrossRef]
15. Derringer, G.; Suich, R. Simultaneous Optimization of Several Response Variables. *J. Qual. Technol.* **1980**, *12*, 214–219. [CrossRef]
16. Zhong, J.; Shi, J.; Shen, J.; Zhou, G.; Wang, Z. Engineering Properties of Engineered Cementitious Composite and Multi-Response Optimization Using PCA-Based Taguchi Method. *Materials* **2019**, *12*, 2402. [CrossRef] [PubMed]
17. *IS 10262*; Concrete Mix Proportioning—Guidelines. BIS (Bureau of Indian Standards): New Delhi, India, 2009; pp. 1–14.

18. Teil, I. Metal Scaffolding. *Policy*, March 2003. Available online: https://allcivilstandard.com/wp-content/uploads/2019/02/BS-01139-5-1990-1998-HD-1000-1988.pdf (accessed on 12 October 2023).
19. Noorvand, H.; Ali, A.A.A.; Demirboga, R.; Noorvand, H.; Farzadnia, N. Physical and chemical characteristics of unground palm oil fuel ash cement mortars with nanosilica. *Constr. Build. Mater.* **2013**, *48*, 1104–1113. [CrossRef]
20. Saini, G.; Vattipalli, U. Assessing properties of alkali activated GGBS based self-compacting geopolymer concrete using nano-silica. *Case Stud. Constr. Mater.* **2020**, *12*, e00352. [CrossRef]
21. Zeng, W.; Zhao, Y.; Zheng, H.; Sun Poon, C. Improvement in corrosion resistance of recycled aggregate concrete by nano silica suspension modification on recycled aggregates. *Cem. Concr. Compos.* **2020**, *106*, 103476. [CrossRef]
22. Sobolev, K.; Ferrada Gutierrez, M. How Nanotechnology Can Change the Concrete World. *Am. Ceram. Soc. Bull.* **2014**, *84*, 113–116.
23. Aghdasi, P.; Heid, A.; Chao, S.-H. Developing Ultra-High-Performance Fiber-Reinforced Concrete for Large-Scale Structural Applications. *ACI Mater. J.* **2016**, *113*, 559–570. [CrossRef]
24. Shoukry, H. Development of Nano Modified Eco-Friendly Green Binders for Sustainable Construction Applications. *Nano Hybrids Compos.* **2019**, *24*, 25–36. [CrossRef]
25. Oyebisi, S.; Ede, A.; Olutoge, F.; Ngene, B. Assessment of activity indexes on the splitting tensile strengthening of geopolymer concrete incorporating supplementary cementitious materials. *Mater. Today Commun.* **2020**, *24*, 101356. [CrossRef]
26. Fallah, S.; Nematzadeh, M. Mechanical properties and durability of high-strength concrete containing macro-polymeric and polypropylene fibers with nano-silica and silica fume. *Constr. Build. Mater.* **2017**, *132*, 170–187. [CrossRef]
27. Shebl, S.; Allie, L.; Morsy, M.; Aglan, H. Mechanical behavior of activated nano silicate filled cement binders. *J. Mater. Sci.* **2009**, *44*, 1600–1606. [CrossRef]
28. Farajzadehha, S.; Mahdikhani, M.; Ziaie Moayed, R.; Farajzadehha, S. Experimental study of permeability and elastic modulus of plastic concrete containing nano silica. *Struct. Concr.* **2020**, *23*, 521–532. [CrossRef]
29. Zhu, Y.; Ju, J.-W. Interface energy effect on effective elastic moduli of spheroidal particle-reinforced nanocomposites. *Acta Mech.* **2020**, *231*, 2697–2709. [CrossRef]
30. Atewi, Y.R.; Hasan, M.F.; Güneyisi, E. Fracture and permeability properties of glass fiber reinforced self-compacting concrete with and without nanosilica. *Constr. Build. Mater.* **2019**, *226*, 993–1005. [CrossRef]
31. Wang, Y.; Zhang, H.; Geng, Y.; Wang, Q.; Zhang, S. Prediction of the elastic modulus and the splitting tensile strength of concrete incorporating both fine and coarse recycled aggregate. *Constr. Build. Mater.* **2019**, *215*, 332–346. [CrossRef]
32. Chu, H.; Wang, Q.; Gao, L.; Jiang, J.; Wang, F. An Approach of Producing Ultra-High-Performance Concrete with High Elastic Modulus by Nano-Al_2O_3: A Preliminary Study. *Materials* **2022**, *15*, 8118. [CrossRef]

Disclaimer/Publisher's Note: The statements, opinions and data contained in all publications are solely those of the individual author(s) and contributor(s) and not of MDPI and/or the editor(s). MDPI and/or the editor(s) disclaim responsibility for any injury to people or property resulting from any ideas, methods, instructions or products referred to in the content.